Design and Implementation of a Peristaltic Pump Based on an Air Bubble Sensor

Huda Farooq Jameel*, Mustafa F. Mahmood, Suhair M. Yaseen

Department of Medical Instrumentation Techniques Engineering
Electrical Engineering Technical College, Middle Technical University
Baghdad, Iraq
E-mails: huda_baban@mtu.edu.iq, mustafa_falah@mtu.edu.iq, suhair.yaseen@mtu.edu.iq

**Corresponding author*

Received: December 14, 2021 **Accepted: October 10, 2022**

Published: December 31, 2022

Abstract: *Peristaltic pumps (PPs) are used to pump clean/sterile or exceptionally responsive liquids without tainting them. They are used in haemodialysis and heart-lung machines to circulate blood as a sidestep during medical procedures. The purpose of this research is to design and construct a PP which consists of a three-roller pump, a bubble sensor, a motor drive, a stepper motor, a microcontroller, and a safety unit. The safety unit functions by using the air bubble sensor, which stops the motor in case of bubble insertion. The performance is experimentally tested in terms of average sensitivity, specificity, and accuracy, which are 99%, 99.55%, and 99.33%, respectively. The evaluation is based on the classification models of true positive (TP), false positive (FP), true negative (TN), and false negative (FN). The overall accuracy is about 98.9%, which indicates the high efficiency of the constructed mechanism.*

Keywords: *Accuracy, Air bubble sensor, Microcontroller, Peristaltic pump, Stepper motor.*

Introduction

The term "peristalsis" comes from the Greek word "peristaltikos", which means compressing and expanding. Peristaltic pumps are used to pump variable fluids without contamination for different purposes of blood circulation during bypass surgery [4], analytical chemistry testing [28], etc. Peristalsis consists of rhythmic, symmetrical contraction and expansion of muscular fibres and is responsible for the pumping of physiological fluids through different parts of the human body [2]. Improvements in peristaltic pump systems have resolved many issues like accuracy, safety, and controlling by a microcontroller. The state-of-the-art of peristaltic pump systems in biomimetics and living nature is presented in [5], allowing for a comparison by showing the structural and functional differences. The developed biomimetic pumping systems mimic the biological principle, thus making use of its advantages. They also show the suitability of this principle in different pumping applications and the sector of medical research. A muscle-powered micro pump providing peristaltic transport is proposed in [26]. *Drosophila melanogaster* larvae that express channelrhodopsin 2 (ChR2) have been used on the cell membrane of skeletal muscles for the acquisition of light-responsive muscle tissues. The authors have obtained peristaltic pumps from the larvae by dissecting them into tubular structures and have found out that the contractions of these tubular structure may be regulated with blue light stimulation. By putting microbeads in the peristaltic pump, the researchers have managed to visualize the internal flow and register the transportation function of the pump. The authors of [15] have created a soft dielectric elastomer peristaltic pump (DEPP). Each of the two pump modules in this DEPP is made up of four layers of dielectric elastomer membrane and three layers of carbon grease as electrodes. The modules are driven by two complimentary signals with four different waveforms: square, sine, saw tooth, and triangular. To characterize the efficiency of the DEPP, the researchers have constructed a measurement system that includes pressure and flow rate sensors. According to their findings, the square wave voltage results in the greatest flow rate and pressure difference in comparison to the other three waveforms. A new form of peristaltic pump, capable of transmitting high-viscosity and solid-liquid mixed fluids with successfully avoiding the difficulties, is offered in [27]. This innovative pneumatic artificial muscle-driven peristaltic pump not only takes less space in the transportation system, but also plays a larger part in pipeline transportation, assuming that its transportation efficiency can be managed.

The current article aims to present the following contributions to the field of peristalsis research:

- A peristaltic pump with an air bubble sensor has been designed and developed.
- Control of the peristaltic pump using an algorithm with a safety unit (in case of bubble insertion in the way of fluids) is taken into consideration in the proposed system.
- The performance of the proposed system is measured, based on sensitivity and specificity as well as performance accuracy information about the total peristaltic pump work.

Related work

Many kinds of research involve several techniques for operating peristaltic pumps with utilizing simulated programmes, such as the model presented in [16], which incorporates structural analyses of a numerically simulated hyper-elastic tube-wall medium. The numerical solutions result in stress and mechanical deflection distributions. The fluid flow produced by the peristaltic pumping activity is computed, and multiple algebraic equation fits are offered, using numerical details regarding the volume change in the interior of the tube.

A robust fluid simulation tool to improve the geometry of the peristaltic pump has been developed in [6]. A comparison between the simulation cyclic pressure results and the experimental ones has shown that they agree well with each other. After matching the simulated pressure magnitudes, the maximum difference evaluated between numerical and experimental data is found to be lower than 5%. Hence, another possible application of the tool is the geometric optimization of pump housing, roller, and hose parts for developing pressure peak optimized pumps.

The authors of [23] explore the possibilities of newly-developed peristaltic rotary pumps for real drug delivery applications. The performances of the proposed two prototypes are reported for different rotation speeds and lag times between consecutive infusions. The presented pumps have shown a good volumetric precision without any dependency on rotation speed and lag time. Moreover, the median and average values of the dosing resolution have been found to be in good accordance with theoretical calculations. The researchers have confirmed the dependability, accuracy, and adaptability of the suggested pumps for intermittent operation and diverse rotation speed conditions. The reported results may lead to an efficient intermittent use of peristaltic pumps in a wide variety of medical applications, including the integration of devices for accurate release of drugs and hormones.

Also, a new type of liquid pump is presented in [21]. The drive of this pump is based on the physical properties of the magnetic fluid or the magnetoelastic properties of the solid structures. The suction and discharge effect of the pump provides a running magnetic wave. The authors describe the pump both in linear and circular arrangement. This new type of pump has certain advantages over the existing ones. However, it requires a two-phase (or multiphase) power supply with a low output frequency or with an adjustable frequency.

An alternative peristaltic pump that can be made by 3D printing and easily accessible off-the-shelf components in most research facilities has been introduced in [13]. In areas like drug screening and test development as well as laboratory-on-the-chip applications and cell culture, such a system has the potential to be disruptive, as hardware costs would be reduced significantly, and more comprehensive fluid systems could be constructed at a fraction of current costs.

A novel peristaltic pump that stimulates the tube by a circulating eccentric oscillation is presented in [18]. The pump characteristics are notably different from standard roller pumps and incorporate continuous flow and configurable flow pulses. The non-occlusive pump can lower the flow pulsation by about 85%, compared to a typical roller pump. The controlled oscillation amplitude enables programmable flow pulsation. This feature allows for generating defined volume flow pulses. For example, pulse forms of a second-generation vessel in the human arterial network can be generated in experimentally.

Different techniques are developed for measuring instantaneous flow fluctuations, e.g. the one demonstrated in [20] – by means of an optical flow sensor using a Bragg fibre-grating sensor and illumination from a 565 nm Light-emitting-diode. The authors have described for the first time a means to continuously measure intrapulse blood flow, using a fibre optic sensor which has the potential to advance monitoring in a medical setting. Further research is necessary to determine how the sensor will behave under more physiological conditions and to study different encapsulations so as to comply with human safety.

Yet another novel invention, the VENTRIFLO True Pulse Pump, which is the first to mimic physiologic pulsatile flow during cardiopulmonary bypass, is studied in [22]. The pump has been shown to generate physiologic pulsatile flow, maintain adequate perfusion of each organ, and provide better systemic O_2 extraction during a 6-h cardiopulmonary bypass pump run. The potential benefits of improved microcirculatory perfusion with pulsatile flow are still to be assessed.

Furthermore, the authors of [3] have developed a highly-customizable kit to build a micro peristaltic pump, which is comprised of 3-D-printed off-the-shelf components. They present two pump variations with different sizes and operating flowrates, which have been constructed using the kit. The latter is designed with modular elements (i.e. each one follows a standardized unit) so as to achieve (1) adaptability (users can easily reconfigure different elements to comply with their experiments); (2) compatibility to progress (new parts with the standardized unit can be developed and effectively interfaced to the current kit) and (3) easy substitution of wear-and-tear components.

Additionally, a linear peristaltic pump, which has been designed and modelled, is illustrated in [17]. The pump is controlled by a set of five electromagnetic actuators with ferromagnetic cores, which press in a specified order an elastic tube with pumped liquid. The researchers display and discuss the fundamental layout of the device, demonstrate its mathematical model and numerical solution, and compare chosen simulation findings with experimental data measured on its prototype. Further research that is focused on the numerical solution of the whole model would enable the identification of the dependence between the field of elasticity and flow needed for the more precise measurement of the pumped liquid.

The authors of [7] have built an occlusion quantification system that generates the flow channel shape in a covered tube from red density images and have corroborated the accuracy of the system. A camera is used to acquire red optical density images within the occluded tube and to create a tube flow channel form through a formula manipulation system. A new degree of occlusion methodology has been used to clarify blood damage caused by the roller pumps employed in CPB. This technique has enabled building high precision three-dimensional forms for locations in the tuber flow channel with a tight gap and to acquire quantitative indications for the assessment of occlusion levels. Micro machined flow sensors which offer suitable functions that enable the application in biosensors of microfluidic systems are discussed in [25]. The most recently explored flow devices are those based on the principle of heat transfer. In [25] a thermal anemometry-based mini-sensor is employed for measuring the velocity of the flow produced by a mini-pump in roller bases. Two elements – a heating one and a temperature monitoring one – are included in the detection unit. Temperature compensation is established, and the instantaneous flow velocity is obtained from the sensor output voltage measurement. The sensor has been defined and positioned in the normal direction to the flow.

Comparative research has been carried out in a big, tertiary hospital in the southeast United States. Observation during medicine administration (medication administration errors, interruptions, programming time), dosage error reduction system (DERS) compliance, and compliance with manufacturer setup criteria have all been used to assess safety and usefulness [19]. Microfluidics and portable systems are discussed, as well as several approaches for making flow-injection measurements. The developed applications mostly address the measurement of inorganic as well as the speciation analysis of various elements and the calculation of multiple overall water quality indicators. Changing the style of manual operations for flow-injection determination usually improves a variety of operational factors, such as detection limits, sampling rate, and selectivity in different matrices [24]. A simple, valve-free, manual roller pump (MRP)-driven microfluidic device has been offered for sequential solution exchange, followed by a protein bioassay. The manual roller pump, which is just a hollow silicone tube with a tiny cylindrical stiff roller, can be a low-cost alternative to pressure-driven pneumatic or syringe pumps that rely on expensive and bulky external equipment; consequently, this approach addresses cost and mobility concerns [21].

The research has classified several related studies based on investigation and comparison of previously developed peristaltic pumps, which are classified below, according to their number of rollers, control method, and accuracy, as shown in Table 1.

This research addresses the problems and applies solutions with an air bubble sensor to detect the bubbles, using an algorithm with a safety unit in the proposed system. The evaluation of the system is measured, based on sensitivity and specificity as well as performance accuracy information for the total peristaltic pump work.

Table 1. Comparison of previously developed peristaltic pumps

Reference	Number of roller	Control method	Acc
[5], 2019	Three	N.A.	N.A.
[6], 2017	N.A.	N.A.	N.A.
[7], 2019	N.A.	Computer	N.A.
[8], 2021	N.A.	Simulation	N.A.
[9], 2019	One	Simulation	N.A.
[10], 2019	Four & five	Computer and microcontroller	N.A.
[11], 2018	Four	Magneto elastic	N.A.
[12], 2020	Six	SOFT-EXE-DMX-J-SA-12300, Arcus Technology	N.A.
[13], 2020	Coupler	N.A.	85%
[14], 2019	Two	Computer and sensor units	N.A.
[15], 2018	N.A.	VENTRI-FLO	N.A.
[16], 2021	Six	Computer and microcontroller	N.A.
[17], 2019	N.A.	N.A.	N.A.
[18], 2020	One	Microcontroller	N.A.
[19], 2018	Three	Microcontroller	N.A.
N.A.: Not available; Acc: Accuracy			

Materials and methods

System design

The proposed system involves a power supply, a DC motor drive, a DC motor, a roller, a tube, a microcontroller, and a bubble sensor, as shown in Fig. 1. The power supply equips both the motor controller and the microcontroller for the purpose of operating the remaining parts. The motor contains three rollers, and within them there is a rubber tube through which the liquid passes. The movement of the motor and the bubble sensor can be controlled by the microprocessor. The purpose of the bubble sensor is to detect bubbles inside the rubber tube. The processor will stop the motor from working with an alarm circuit that is designed to stop the motor in case an air bubble passes through the liquids pathway. The practical components of the system are shown in Fig. 2.

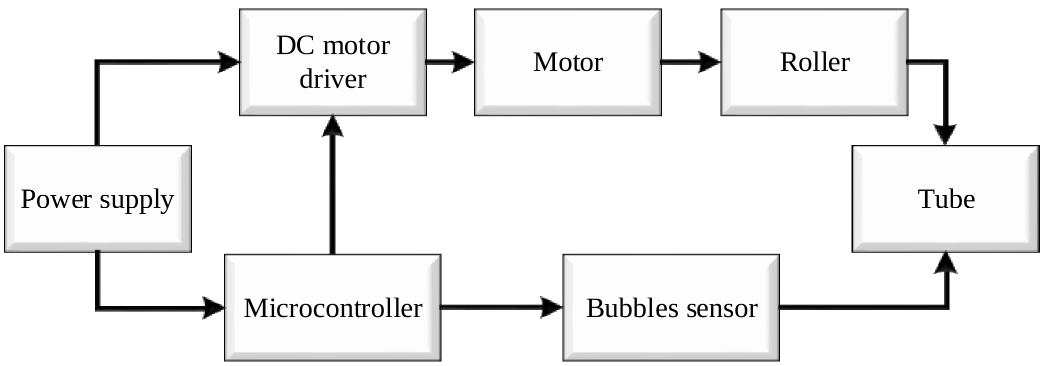

Fig. 1 Block diagram of pump system

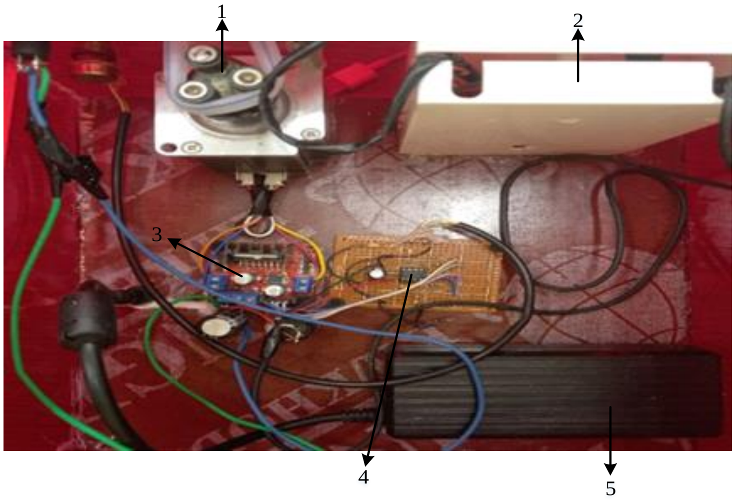

Fig. 2 Practical components of pump system: 1 – Rotary motor, 2 – Protection unit, 3 – Motor drive, 4 – Microcontroller (PIC12F675), and 5 – Power supply

Bubble detector

As shown in Fig. 3 and Fig. 4, the bubble sensor is used to stop the motor in case of a bubble passing through the tube. The IR sensor is placed in the way of the fluid tube. The circuit consists of a photo diode and a photo transistor to detect the bubble, and these components are connected to an LM358 operation amplifier. The signal is amplified in case of a bubble insertion to indicate its detection, and the buzzer will be ON to alarm the user and stop the motor at the same time.

Fig. 3 Snap shot of the bubble detector circuit: 1 – Motor, 2 – Photo diode and photo transistor, and 3 – LM358 operation amplifier

PIC12F675 is a microcontroller [8], where pins 1, 5, and 8 are connected to VSS and GND, respectively. Pins 3, 4, 6, and 7 are connected to the motor drive control, i.e. L298N. The motor drive controller board module dual h Bridge DC Stepper [10] and the Bipolar Nema 23 stepper motor with 1.8 deg [11] are used to control the pump work. The circuit of the microcontroller is shown in Fig. 5.

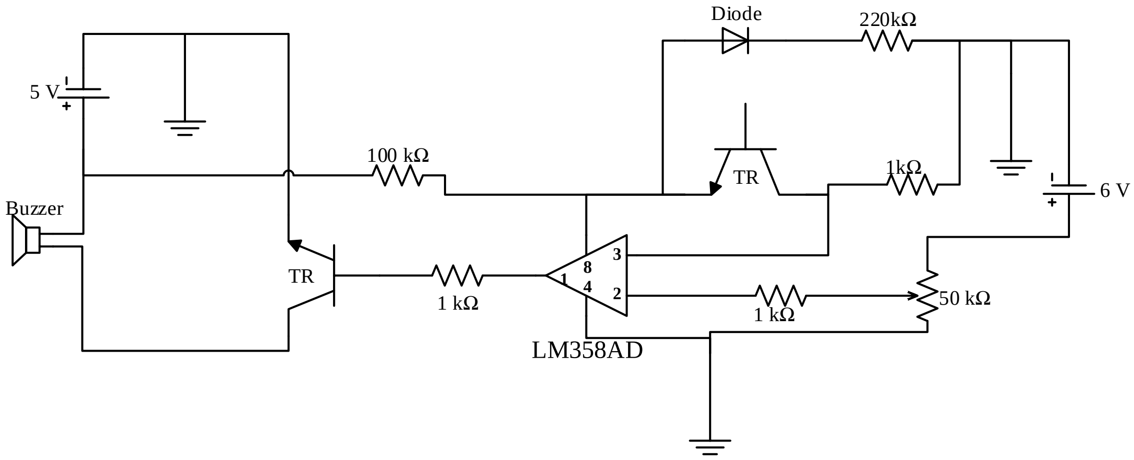

Fig. 4 The detector circuit for air bubbles

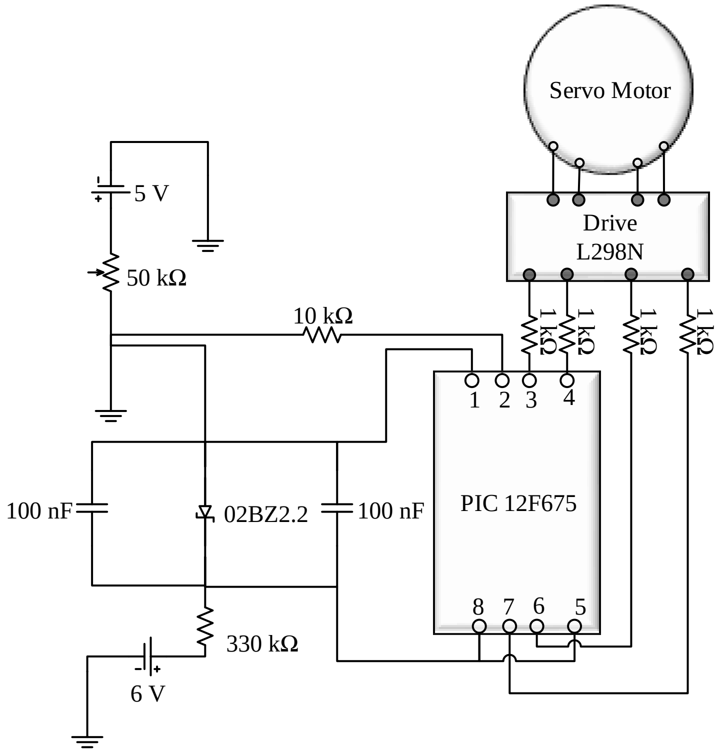

Fig. 5 The circuit for microcontroller connection

Algorithm in case of a bubble

The algorithm in Fig. 6 shows the mechanism of action of the system in the event of an air bubble in the fluid in the pipe. The system starts with a specified speed of the motor's rotation, chosen through the microprocessor; then the liquid passes through the rubber tube within the three rollers in the absence of an air bubble inside the pipe. The motor works continuously, and if a signal is detected by the bubble sensor (i.e. in case of an air bubble), the motor will stop working with an audible alert.

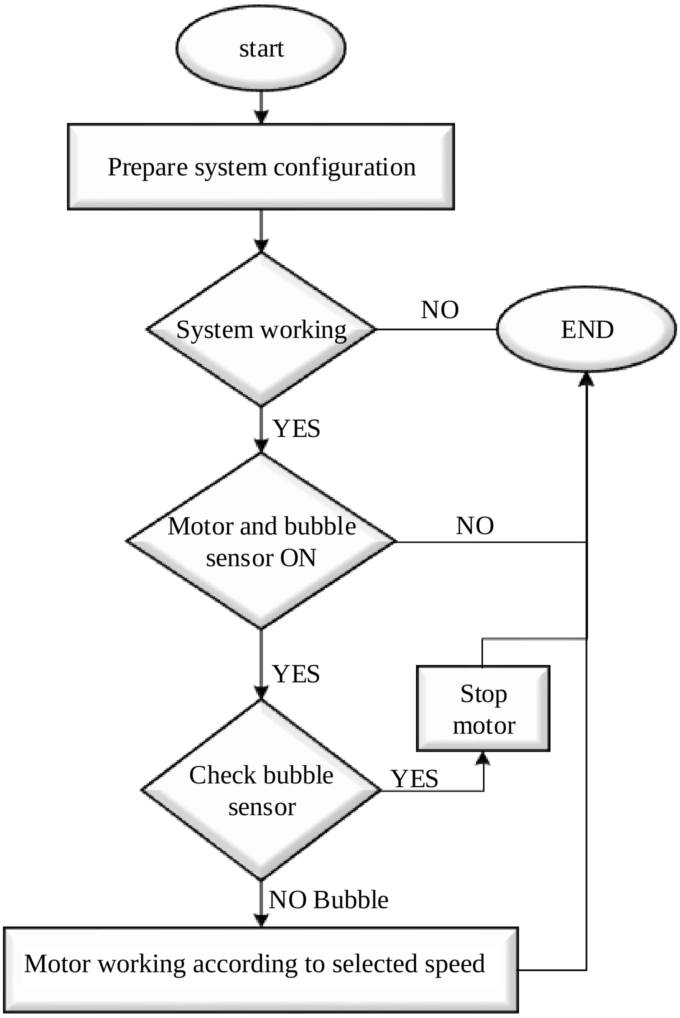

Fig. 6 Algorithm for air bubble detection

The present article demonstrates the code of the system and how the code works using a flow code programme [9] when the circuit is ON. The motor is programmed in two speeds for controlling the flow of the fluid (blood). When the programme starts, port A is used as a connection between the microcontroller and the motor driver. Also, a "call macro" component is used to write the equation for control of the motor speed, and the system output is used to get the response. Finally, delay is used to control the rotation of the motor.

Performance classification

The classification of the system performance has been derived from three statistical analyses, namely sensitivity, specificity, and accuracy [12]. These measurements are based on four indices that have four possible attempts, which are: true positive (*TP*), when the motor is in ON position, and the bubble sensor is active; false positive (*FP*), when the motor is in OFF position, and the bubble sensor is active; true negative (*TN*), when the motor is in ON position, and the bubble sensor is not active; and false negative (*FN*), when the motor is in OFF position, and the bubble sensor is not active. Sensitivity (*SN*) refers to the ability of the system to perform its functions (sensitivity is also known as recall).

The sensitivity is calculated according to Eq. (1) [12], as follows:

$$SN\% = \frac{TP}{TP + FN} \times 100 \tag{1}$$

The specificity is calculated according to Eq. (2) [12], as follows:

$$SP\ \% = \frac{TN}{TN + FP} \times 100 \tag{2}$$

The accuracy is calculated according to Eq. (3) [12], as follows:

$$AC\ \% = \frac{TP + TN}{Pn + Nn} \times 100 \tag{3}$$

Pn and *Nn* denote the number of positive and negative attempts, respectively. To evaluate the overall system accuracy, *F-measure accuracy* has been computed to evaluate the overall performance [14]. *F-measure accuracy* represents the combination of recall (sensitivity) and precision, which is defined as follow:

$$Precision\ \% = \frac{TP}{TP + FP} \times 100 \tag{4}$$

$$F\text{-}measure\ accuracy\ \% = 2 \times \frac{recall \times precision}{recall + precision} \times 100 \tag{5}$$

Results and discussion

In this section, the results are presented in two parts regarding the safety unit and the evaluation of the system performance. Moreover, validated measurements of the proposed system are investigated statistically (i.e. in terms of accuracy, sensitivity, and specificity).

Safety unit

This section indicates the effect of the protection unit on the system, which is illustrated in Fig. 7. It demonstrates that the motors will continue to move in the absence of bubbles, and in case of bubble insertion in the tube, the motors will be OFF and the system will stop. The motors will start working again at the selected speed when there are no longer bubbles in the tube.

Performance results of the system

In this section, the performance results of the system are discussed, based on the classification models: *TP*, *FP*, *TN*, and *FN*. These classification models are illustrated in Tables 2 and 3. All test cases are carried out by repeating (100, 200, and 300). The experimental evaluations are summarized in Table 2 and 3.

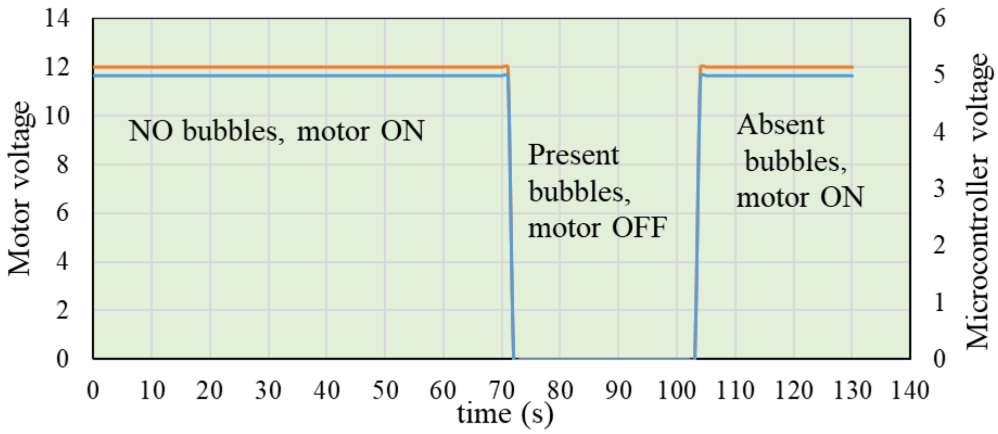

Fig. 7 The mechanism of action of the motor through the bubble sensor

Table 2. Experimental sensitivity evaluation for two test cases (100, 200 attempts)

Test 1	Speed 1	Speed 2
Attempts	100	200
TP	99	198
FN	1	2
Sensitivity, (%)	99	99

Table 3. Experimental specificity evaluation for two test cases (200, 300 attempts)

Test 2	Speed 1	Speed 2
Attempts	200	300
TN	199	299
FP	1	1
Specificity, (%)	99.5	99.6

Accuracy, sensitivity, and specificity are statistically analysed to validate the performance of the proposed system. The average sensitivity, specificity, and accuracy for Test 1 are 99%, 99.55%, and 99.33%, respectively. The overall performance accuracy information is listed in Table 4, and it is estimated to be ≈ 98.9%.

Overall 100 experiments have been carried out. The accuracy validation is expressed as a confusion matrix. The confusion matrix gives a clear illustration for the number of experiments and the accuracy of the system.

Conclusion

This article presents a peristaltic pump with three rollers and bubble sensors, which has been developed and manufactured. The system comprises of power supply, a stepper motor, and PIC12F675, as well as a safety unit. An air bubble sensor is used to halt the motor when a bubble is inserted, and it is used as a safety unit. The IR bubble sensor is composed of a photodiode and a photo transistor, the IR circuit is coupled with a buzzer in ON position.

Table 4. Overall system accuracy

Parameters	Test 1	Test 2
Total number of experiments	100	100
TP	96	97
FP	1	1
TN	2	1
FN	1	1
Confusion matrix $\begin{matrix} TP & FN \\ FP & TN \end{matrix}$	Confusion matrix $\begin{matrix} 96 & 1 \\ 1 & 2 \end{matrix}$	Confusion matrix $\begin{matrix} 97 & 1 \\ 1 & 1 \end{matrix}$
Precision, (%)	98.9	98.9
Recall, (%)	98.9	98.9
F-measure accuracy = $2 \times \frac{\text{recall} \times \text{precision}}{recall + precision} \times 100\ \%$	98.9	98.9
Overall accuracy = 98.9%		

The system performance is tested in terms of the average sensitivity, specificity, and accuracy, which have been found to be 99%, 99.55%, and 99.33%, respectively. The assessment of the system performance is based on *TP*, *FP*, *TN*, and *FN*. The total accuracy of the proposed system is about 98.9%, reflecting excellent efficiency in the manufacturing process. Increasing in the number of pump rollers could be the subject of further research, as it is expected that this will increase streamlining of the liquid flow, reduce the possibility of air bubble insertion, and perform better control on the pump speed. In addition, using power transfer would ensure a long operation time of recharged battery. The use of wireless power transfer is suggested as a future work for direct operation of the system.

Acknowledgements

The authors would like to thank the staff of the Department of Medical Instrumentation Techniques Engineering, Electrical Engineering Technical College, Middle Technical University for their support during this study.

References

1. Biswas G. C., H. Suzuki (2022). Simple Manual Roller Pump-driven Valve-free Microfluidic Solution Exchange System for Urgent Bioassay, RSC Advances, 12(2938-2946), doi: 10.1039/D1RA08052K.
2. Chavan A., A. S. Patil, S. L. NS (2020). Overview of Peristaltic Pump Suitable For Various Slurries and Liquids, Int J Sci Res & Eng Trends, 6(3), 1323-1327.
3. Ching, T., Vasudevan, J., Tan, H. Y., Lim, C. T., Fernandez, J., Toh, Y.-C., & Hashimoto, M. (2021). Highly-customizable 3D Printed Peristaltic Pump Kit, HardwareX, 10, e00202, doi.org/10.1016/j.ohx.2021.e00202.
4. Cohn L. H., D. H. Adams (2017). Cardiac Surgery in the Adult (5th Ed.), New York.
5. Esser F., T. Masselter, T. Speck (2019). Silent Pumpers: A Comparative Topical Overview of the Peristaltic Pumping Principle in Living Nature. Engineering and Biomimetics, Advanced Intelligent Systems, 1(2), 1900009, doi.org/10.1002/aisy.201900009.

6. Formato G., R. Romano, A. Formato, J. Sorvari, T. Koiranen, A. Pellegrino, F. Villecco (2019). Fluid-structure Interaction Modeling Applied to Peristaltic Pump Flow Simulations, Machines, 7(3), 50, doi.org/10.3390/machines7030050.
7. Fukaya A., Y. Shiraishi, Y. Inoue, A. Yamada, G. Sahara, T. Kudo, et al. (2021). Development and Accuracy Evaluation of a Degree of Occlusion Visualization System for Roller Pumps Used in Cardiopulmonary Bypass, J Artif Organs, 24(1), 27-35.
8. https://components101.com/microcontrollers/pic12f675-pinout-datasheet/ (Access Date 15 December 2022).
9. https://flowcode.software.informer.com/4.0/ (Access Date 15 December 2022).
10. https://www.amazon.com/Qunqi-Controller-Module-Stepper-Arduino/dp/B014KMHSW6 (Access Date 15 December 2022).
11. https://www.amazon.com/STEPPERONLINE-Stepper-Motor-179oz-Bipolar/dp/B00QG1ZF48/ref=sr_1_10?crid=23GWHNF6E9LXY&dchild=1&keywords=stepper+motor+kit&qid=1623350488&sprefix=stepper+motor+%2Caps%2C-1&sr=8-10 (Access Date 15 December 2022).
12. Jameel H. F., S. L. Mohammed, S. K. Gharghan (2019). Wheelchair Control System based on Gyroscope of Wearable Tool for the Disabled, The Fourth Scientific Conference for Engineering and Postgraduate Research IOP Conference Series: Materials Science and Engineering, 745(012091), doi: 10.1109/DeSE.2019.00156.
13. Jönsson A., A. Toppi, M. Dufva (2020). The FAST Pump, a Low-cost, Easy to Fabricate, SLA-3D-printed Peristaltic Pump for Multi-channel Systems in Any Lab, HardwareX, 8, e00115, doi.org/10.1016/j.ohx.2020.e00115.
14. Ma C., W. Li, R. Gravina, G. Fortino (2017). Posture Detection Based on Smart Cushion for Wheelchair Users, Sensors, 17(4), 719, doi.org/10.3390/s17040719.
15. Mao G., L. Wu, Y. Fu, Z. Chen, S. Natani, Z. Gou, et al. (2018). Design and Characterization of a Soft Dielectric Elastomer Peristaltic Pump Driven by Electromechanical Load, IEEE/ASME Transactions on Mechatronics, 23(5), 2132-2143.
16. Momenzadeh, N., P. Von Lockette (2021). Modeling and Simulations of a Novel Magnetorheological Peristalsis Blood Pump, Active and Passive Smart Structures and Integrated Systems XV, 11588(11), doi.org/10.1117/12.2585086.
17. Muška J., P. Karban, I. Petrášová, I. Doležel (2019). Design of Linear Peristaltic pump, 2019 IEEE 20th International Conference on Computational Problems of Electrical Engineering (CPEE), doi: 10.1109/CPEE47179.2019.8949082.
18. Pech S., R. Richter, J. Lienig (2020). Peristaltic Pump with Continuous Flow and Programmable Flow Pulsation, IEEE 8th Electronics System-integration Technology Conference (ESTC), doi: 10.1109/ESTC48849.2020.9229731.
19. Penoyer D., K. Giuliano, A. Middleton (2022). Comparison of Safety and Usability Between Peristaltic and Pneumatic Large-volume Intravenous Smart Pumps During Actual Clinical Use, BMJ Innovations, 8, 78-86, doi: 10.1136/bmjinnov-2021-000851.
20. Ruiz-Vargas A., S. A. Morris, R. H. Hartley, J. W. Arkwright (2019). Optical Flow Sensor for Continuous Invasive Measurement of Blood Flow Velocity, Journal of Biophotonics, 12(10), e201900139, doi.org/10.1002/jbio.201900139.
21. Stork M., D. Mayer (2018). Peristaltic Pump with Magnetoelastic Drive, IEEE Transactions on Magnetics, 54(5), 1-4, doi: 10.1109/TMAG.2018.2804331.
22. Sunagawa G., J. H. Karimov, R. Dessoffy, N. Byram, P. Grady, M. Sinkewich, et al. (2018). New Technology Mimics Physiologic Pulsatile Flow During Cardiopulmonary Bypass, J Artif Organs, 42(2), 231-235.
23. Tamadon I., V. Simoni, V. Iacovacci, F. Vistoli, L. Ricotti, A. Menciassi (2019). Miniaturized Peristaltic Rotary Pump for Non-continuous Drug Dosing, 41st Annual

International Conference of the IEEE Engineering in Medicine and Biology Society (EMBC), doi: 10.1109/EMBC.2019.8857811.
24. Trojanowicz M., M. Pyszynska (2022). Flow-injection Methods in Water Analysis – Recent Developments, Molecules, 27(1410), doi: 10.3390/molecules27041410.
25. Xavier A. R., C. S. Moreira, A. G. B. Neto, A. M. Lima, H. Neff, F. W. Diasi (2018). Real-time Flow Monitoring for a Roller-based Peristaltic Mini-pump, IEEE International Instrumentation and Measurement Technology Conference (I2MTC), doi: 10.1109/I2MTC.2018.8409790.
26. Yamatsuta E., S. P. Beh, K. Uesugi, H. Tsujimura, K. Morishima (2019). A Micro Peristaltic Pump Using an Optically Controllable Bioactuator, Engineering, 5(3), 580-585.
27. Yan H., Z. Yang, F. Ding, S. Xu, D. Zhang (2019). Design of a Peristaltic Pump Driven by Pneumatic Artificial Muscles, International Conference on Artificial Intelligence and Security, Lecture Notes in Computer Science, 11634, 266-275.
28. Yaseen S. M., B. B. Qassim, N. O. Al-Lami (2020). Synthesis, Identification, and Using of New Nitro Hydrazone Ligand in Spectrophotometric Quantification of Co(II) Content in Vitamin B12 Injections, Int J Drug Delivery Tech, 10(4), 513-518.

Huda Farooq Jameel
E-mail: huda_baban@mtu.edu.iq

Huda Farooq Jameel works in the Middle Technical University, Electrical Engineering Technical College, Medical Instrumentation Techniques Engineering Department. She received her B.Sc. Degree in Medical Instrumentation Techniques Engineering from the Middle Technical University, Iraq, in 2006. In 2020, she obtained her M.Sc. Degree in Electronic Medical Instrumentation Techniques Engineering. She is interested in biomedical sensors, digital image processing, as well as medical instrumentation design and development.

Mustafa F. Mahmood
E-mail: mustafa_falah@mtu.edu.iq

Mustafa Falah Mahmood received his B.Sc. Degree in Medical Instrumentation Techniques Engineering from the Middle Technical University, Iraq, in 2010. He works at the Department of Medical Instrumentation Engineering Techniques, Electrical Engineering Technical College, Middle Technical University, Baghdad, Iraq, as an Assistant Teacher. He received his M.Sc. Degree in Medical Instrumentation Engineering Techniques, from the Electrical Engineering Technical College, Baghdad, Iraq, in 2020. He is interested in studies that are concerned with wireless energy transmission, alternative energy generation without the use of batteries, the design of medical devices with low cost and high efficiency, biomedical sensors, and microcontroller applications.

Suhair M. Yaseen, Ph.D. Student
E-mail: suhair.yaseen@mtu.edu.iq

Suhair Mohammed Yaseen received her B.Sc. Degree in Chemistry Sciences from the University of Baghdad. She received her M.Sc. Degree in Chemistry Sciences from the same University and currently she is at the last stage of her Ph.D. studies in the field of Analytical Chemistry because of her work in the College of Electrical Engineering Techniques. She is interested in chemistry application medical engineering.